CMS实验格点QCD相关最新进展

Shuo Han

IHEP

CLQCD 2026 · CUHK–Shenzhen

9 October 2026





中国科学院高能物理研究所
Institute of High Energy Physics
Chinese Academy of Sciences

Outline

1 **Heavy-flavour spectroscopy and weak decays**

All-charm structures · B* mass splittings · R(J/ψ)

---

2 **Parton dynamics and hadron formation**

Heavy-quark radiation · gluon spin · quarkonium in jets · $t\bar{t}$ threshold

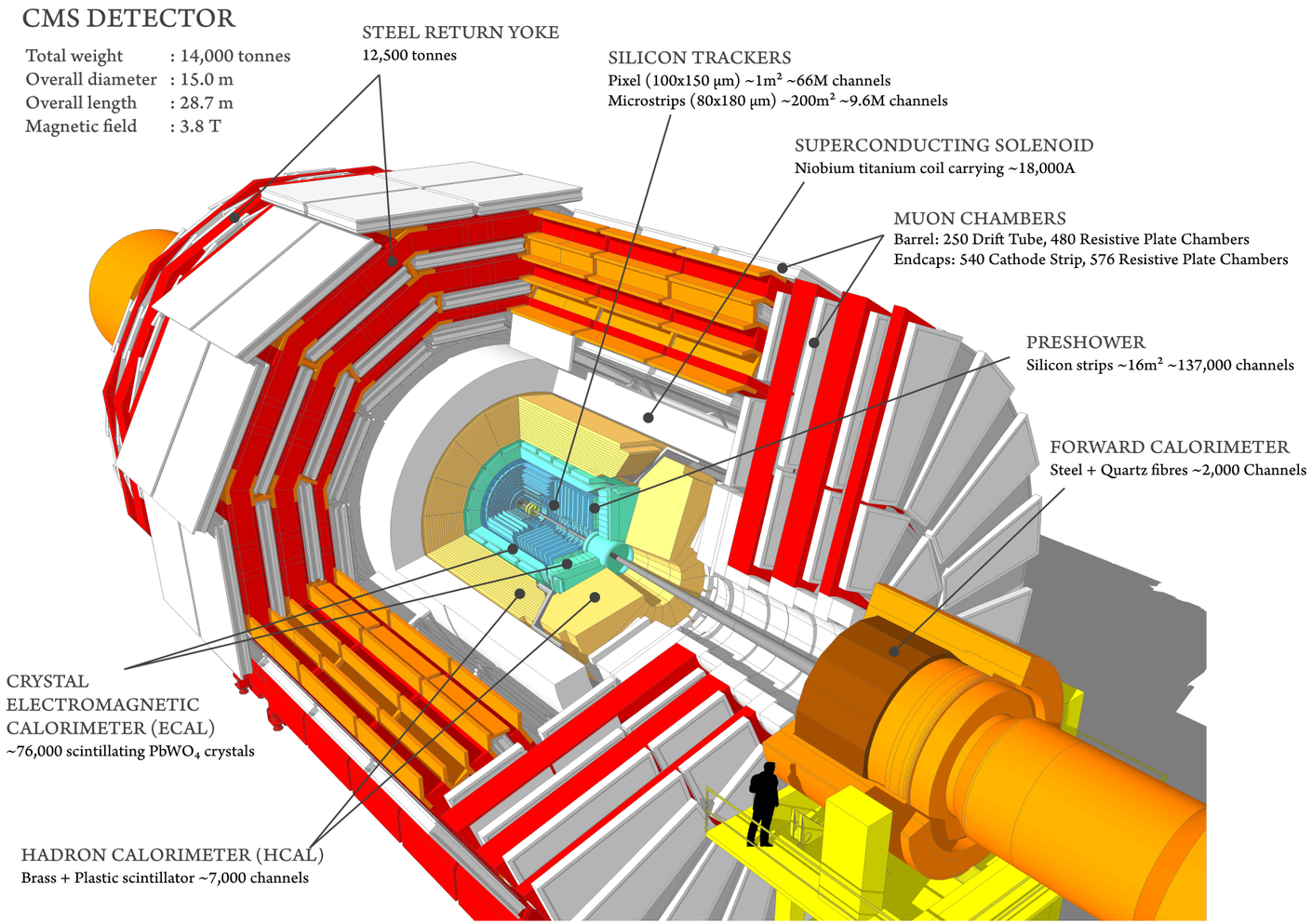
---

3 **QCD matter in light-ion collisions**

Collective flow · bottomonium suppression

Recent CMS experimental highlights, primarily from 2025–2026.

CMS: strengths and experimental constraints



Silicon tracker · ECAL / HCAL · 3.8 T solenoid · muon system

Pros: energy and statistics.

pp data	√s	Recorded
Run 2 · 2015–18	13 TeV	150.8 fb^{-1}
Run 3 · 2022–26	13.6 TeV	326.0 fb^{-1}

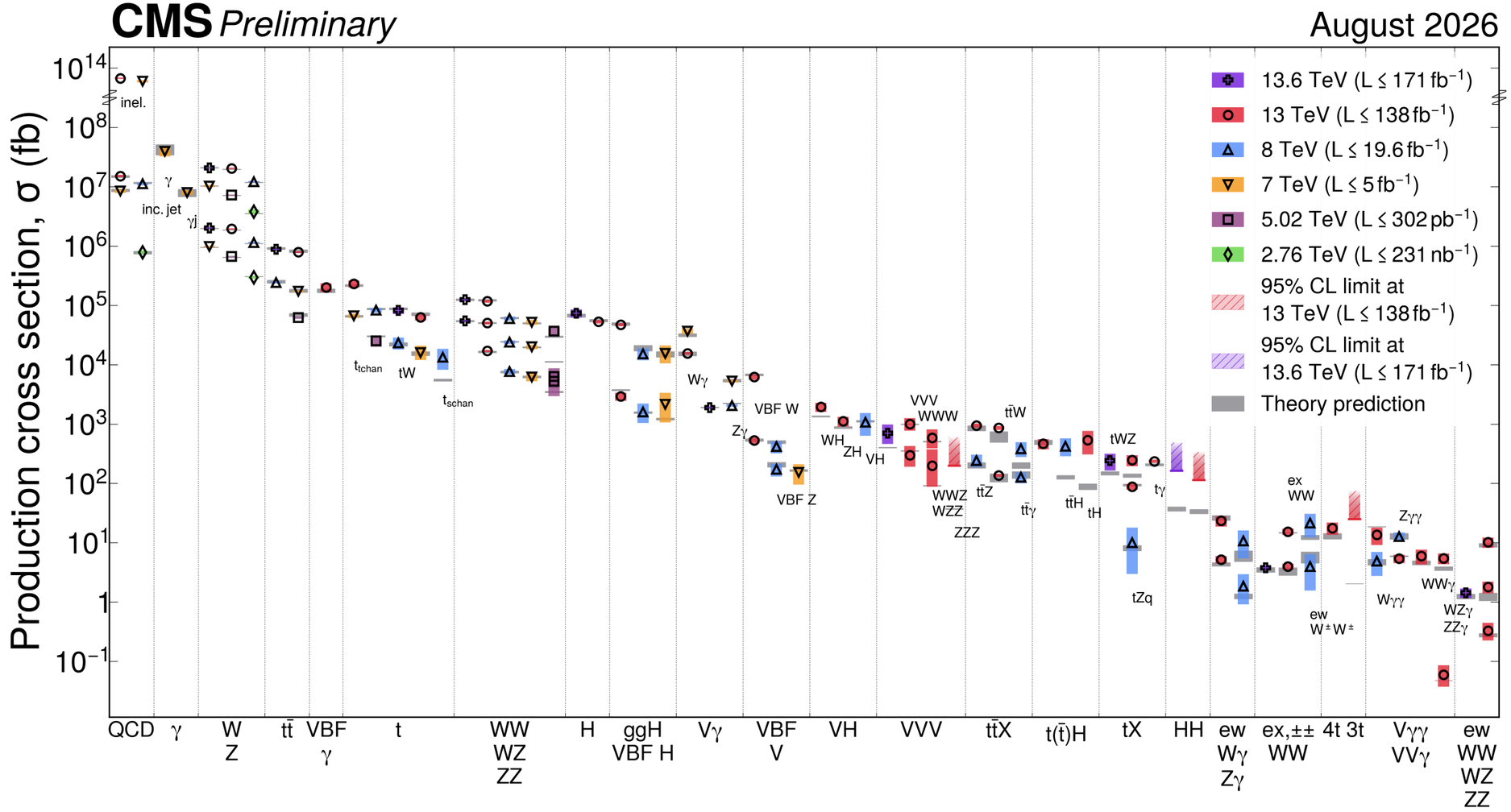
Run 2 + 3: 476.8 fb^{-1} recorded.
Each analysis uses its own selected subset.

Pros: versatile reconstruction.
3.8 T tracking, calorimeters and muons cover leptons, photons, jets and missing momentum.

Cons: rate, pileup and bandwidth.
QCD backgrounds and overlapping vertices complicate reconstruction; triggers limit low-p_T acceptance.

CMS detector: official cutaway illustration · CMS recorded luminosity, Run 2 + Run 3

CMS: from the energy frontier to QCD



Measurements broadly follow the SM over many orders of magnitude in cross section.

[CMS Standard Model summary plots (August 2026)]

Recent CMS heavy-flavour measurements

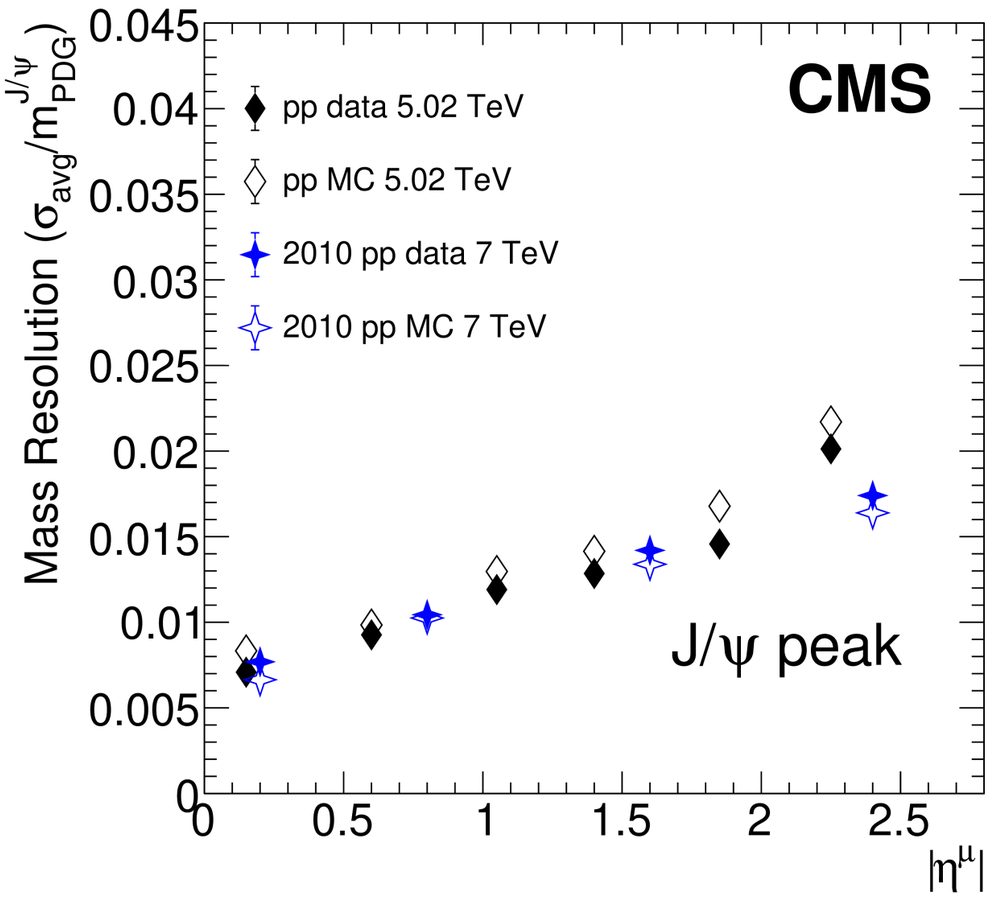
What is measured?	Paper	Paper release
All-charm spin and parity: J^{PC} [a]	Nature 648 (2025) 58	June 2025
All-charm masses, widths and interference J/ψ J/ψ [b] and J/ψ ψ(2S) [c]	arXiv:2602.02252	February 2026
ΔM = M(B*) − M(B) Hyperfine mass splittings for u, d, s	PRL 136 (2026) 031902	August 2025
R(J/ψ): τ / μ decay-rate ratio Lepton universality in $B_c \to J/\psi \ell \nu$	PRD 113 (2026) L111101	October 2025

[a] Spin/parity (2025): Nanjing Normal · Tsinghua · Henan Normal
[b] J/ψ J/ψ PAS (2025): Nanjing Normal · Fudan · Tsinghua · Sun Yat-sen · U. Shanghai for Sci. & Tech. · Henan Normal
[c] J/ψ ψ(2S) PAS (2025): Nanjing Normal · Tsinghua · IHEP · Zhejiang · Henan Normal

Heavy flavour & weak decays | Parton dynamics | QCD matter

Institution notes: analysis / presentation roles listed in the CLHCP2025 report, p. 59.
Paper dates need not be the first public result. Unmarked results are not assigned here.

Muon precision at the charmonium scale



Detector-resolution reference: pp at 5.02 / 7 TeV
The following analyses use 13 / 13.6 TeV data.

J/ψ and ψ(2S): $c\bar{c}$ mesons
Their $\mu^+\mu^-$ decays provide a clean tag; tracking determines the mass resolution.

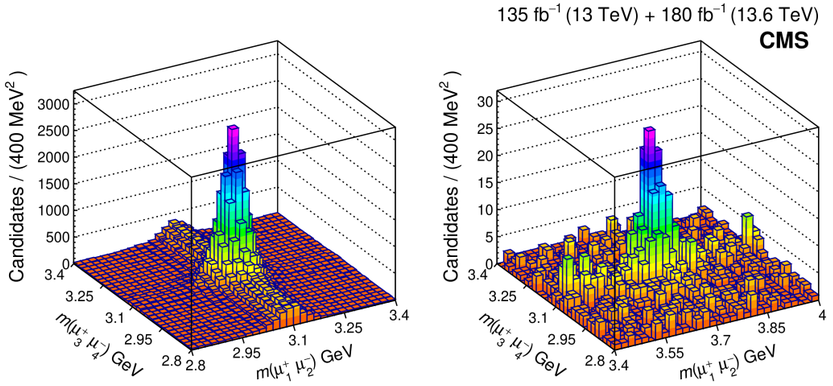
J/ψ mass resolution in data
$\sigma(m_{\mu\mu})/m \approx 0.7–2\%$, depending on η.
About 20 MeV in the central region.

The four-muon analyses reach
$p_T^{\mu} > 2$ GeV, $|\eta^{\mu}| < 2.4$;
trigger acceptance is more restrictive.

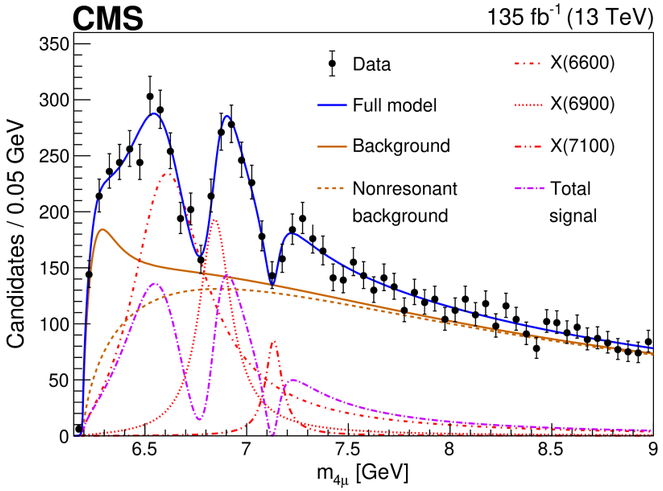
J/ψ mass constraints sharpen $m_{4\mu}$.

CMS, JINST 19 (2024) P09012, Fig. 17a · Four-muon selection: arXiv:2602.02252

From muons to a double-charmonium sample



J/ψ J/ψ (left) · J/ψ ψ(2S) (right, tighter selection)
Real pairs form peaks in both dimuon masses.



Run 2 · 135 fb^{-1} · 13 TeV

2020 · LHCb: X(6900).
2022 · CMS: three structures;
the third was then evidence.

Now: spin, interference and a second decay channel.

Muon triggers retain the events

Run 2: dedicated μ paths
Run 3: add dimuon parking

↓

Kinematic + muon-ID cuts

≥4 soft-ID μ: p_T > 2 GeV, |η| < 2.4
Opposite-charge pairs: $p_T^{J/\psi}$ > 3.5 GeV

↓

Suppress random dimuon pairs

J/ψ mass windows + vertex-fit quality;
mass constraints sharpen $m_{4\mu}$.

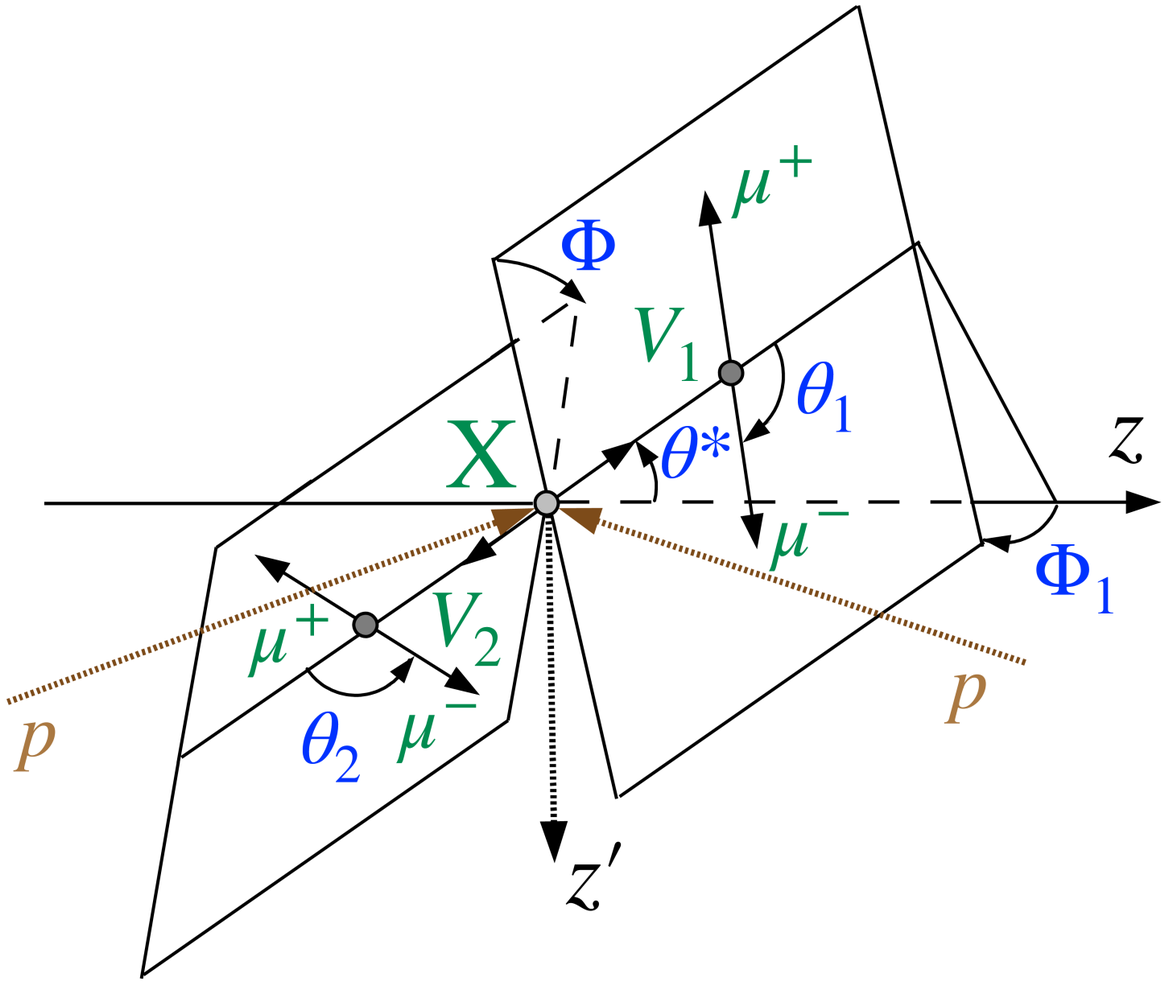
↓

Mass and angular fits

$m_{4\mu}$: X(6600), X(6900), X(7100)
Decay angles: spin / parity

History: LHCb (2020) · CMS PAS (2022) · Run 2 fit: Nature 648 (2025) 58, Fig. 1
Pair reconstruction and selection: CMS, arXiv:2602.02252, Methods and Fig. 2

2025: spin from the two J/ψ decay planes



X → J/ψ J/ψ → (μ⁺μ⁻)(μ⁺μ⁻) · 135 fb⁻¹, Run 2

Challenge: acceptance and continuum production distort the measured angles.

θ_1, θ_2, Φ → probabilities P_i

$\theta_{1,2}$: μ^- helicity angles

Φ: angle between the decay planes

↓

$D_{ij} = P_j / (P_i + P_j)$

Matrix-element probabilities

↓

Fit mass and the angular discriminant

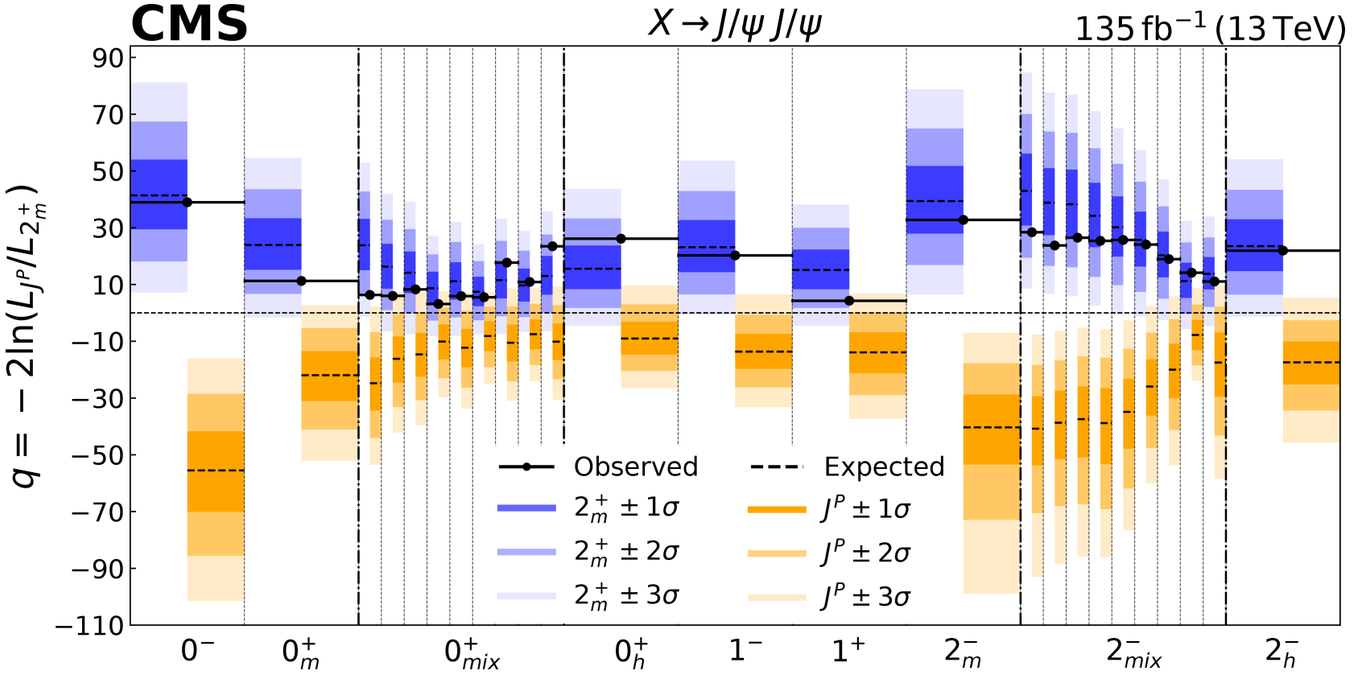
Simulation accounts for detector acceptance

High-mass data test the continuum model

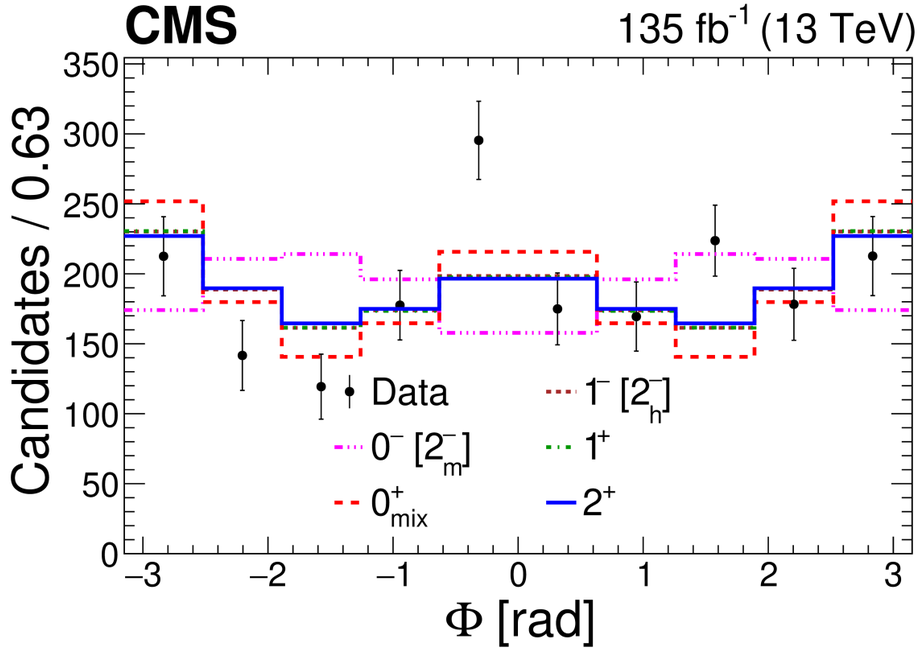
Compare the spin–parity hypotheses

CMS, Nature 648 (2025) 58 · arXiv:2506.07944, Fig. 5

2025: the first all-charm quantum-number measurement



Black: observed test statistic
Blue: 2^+ model · orange: alternative hypotheses



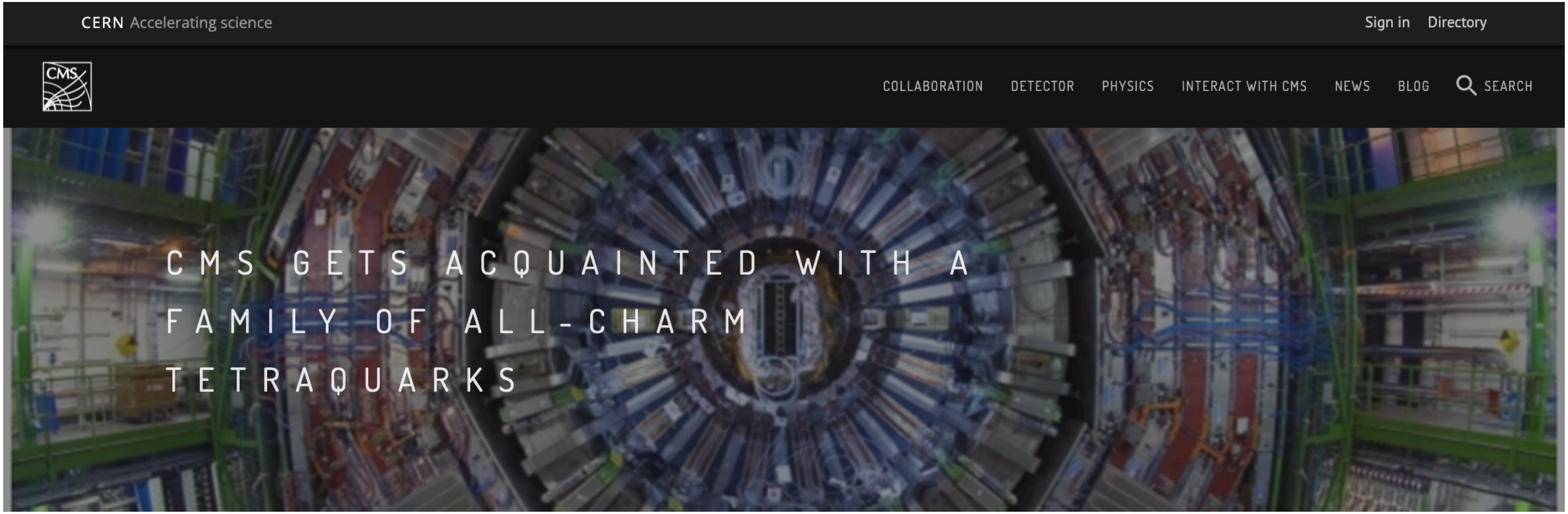
Decay-plane angle Φ · background subtracted
Systematic uncertainties not shown

Common $J^{PC} = 2^{++}$ favoured
J = 0 excluded at 95% CL
J = 1 excluded at 99% CL

Likelihood-ratio tests calibrated with pseudoexperiments.
Common quantum numbers and decay structure assumed; no separate assignment to each peak.

CMS, Nature 648 (2025) 58 · arXiv:2506.07944, Figs. 4 and 6a

CMS physics briefing: all-charm spin and parity



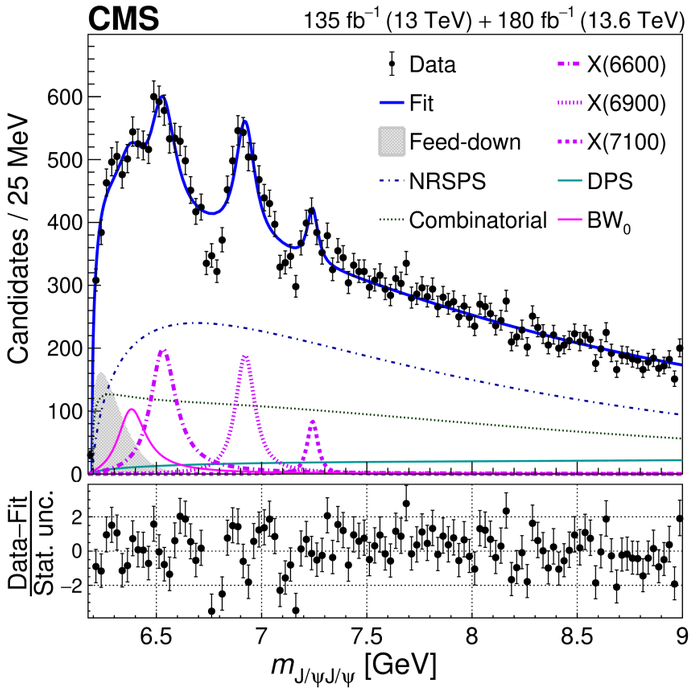
CMS official news · 3 December 2025

Result published in **Nature 648 (2025) 58**

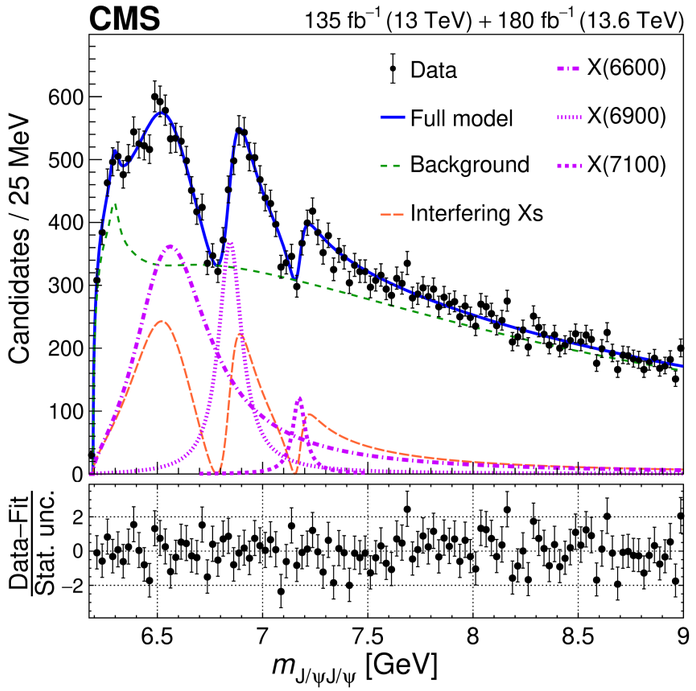
Run 2 + Run 3: peaks and interference

135 + 180 fb^{-1} · 3.6× Run 2 yield · all three structures >5σ · X(7100): 7.7σ

Signal $\propto |a_1\,BW_{6600} + a_2\,BW_{6900} + a_3\,BW_{7100}|^2$ · complex a_i; continuum added separately



Noninterfering model

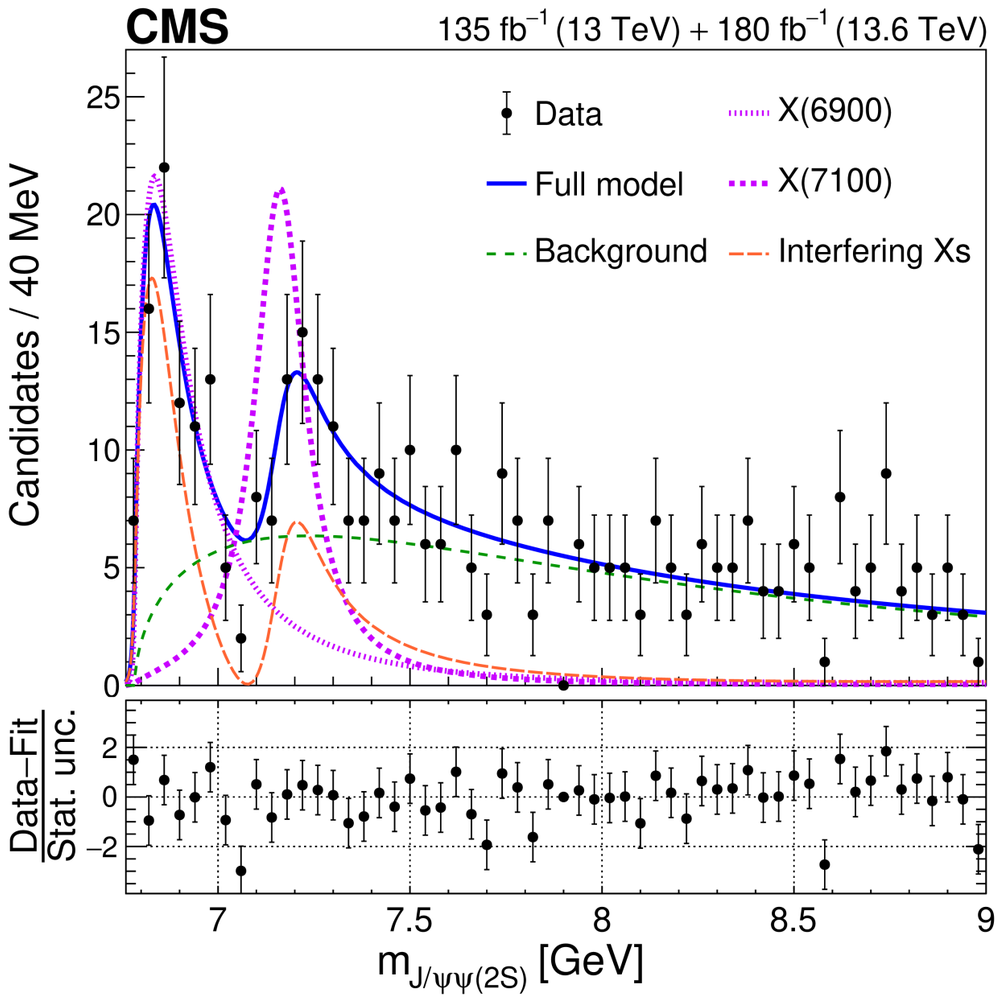


Coherent model

Interference >5σ: peaks and dips constrain amplitudes and phases.

First public: CMS PAS (April 2025) · Updated paper: arXiv:2602.02252 (2026), Figs. 10 and 3

Another channel: J/ψ ψ(2S)



J/ψ ψ(2S) → 4μ · Run 2 + Run 3

Smaller ψ(2S) → μμ rate, more background.
Use harder charmonium-p_T cuts, optimized on Run 2 data.

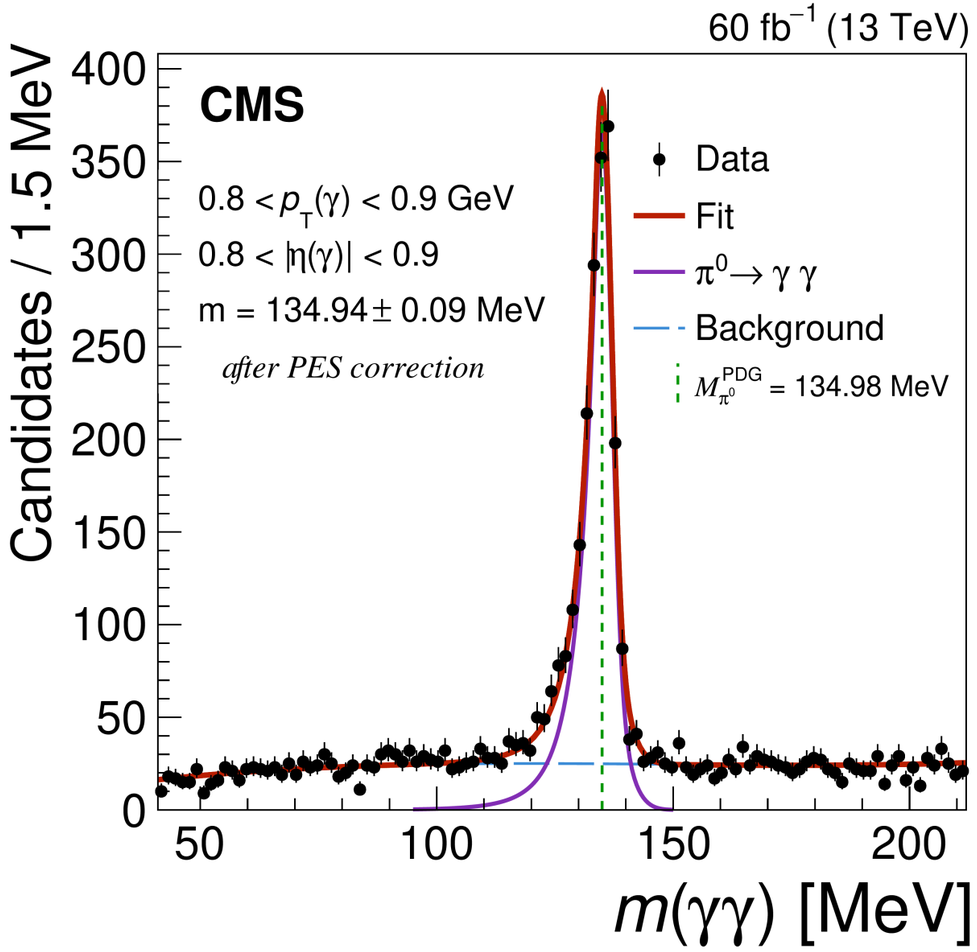
Veto alternative double-J/ψ pairings; fit the J/ψ ψ(2S) invariant mass.

X(6900): >8σ · X(7100): >4σ
Interference: 2.5σ.
Consistent with a diquark picture; not a unique structural interpretation.

ATLAS (2025): X(6900) at 8.9σ in 4μ and 4μ + 2π; no significant structure near 7.2 GeV.

CMS, arXiv:2602.02252 (2026), Fig. 4 · ATLAS, PRD 113 (2026) 112015

Soft photons: conversion tracks and π^0 calibration



$\pi^0 \rightarrow \gamma\gamma$, both $\gamma \rightarrow e^+e^-$ · after momentum calibration
Shown: p_T^γ = 0.8–0.9 GeV, $|\eta^\gamma|$ = 0.8–0.9

$B^*(1^-) \rightarrow B(0^-) + \gamma$

Same $q\bar{b}$ content, q = u, d, s

E_γ^* ≈ 40–50 MeV in the B* rest frame

↓

Boost + photon conversion

$\gamma \rightarrow e^+e^-$ in detector material

Tracking reaches $p_T^\gamma > 0.3$ GeV

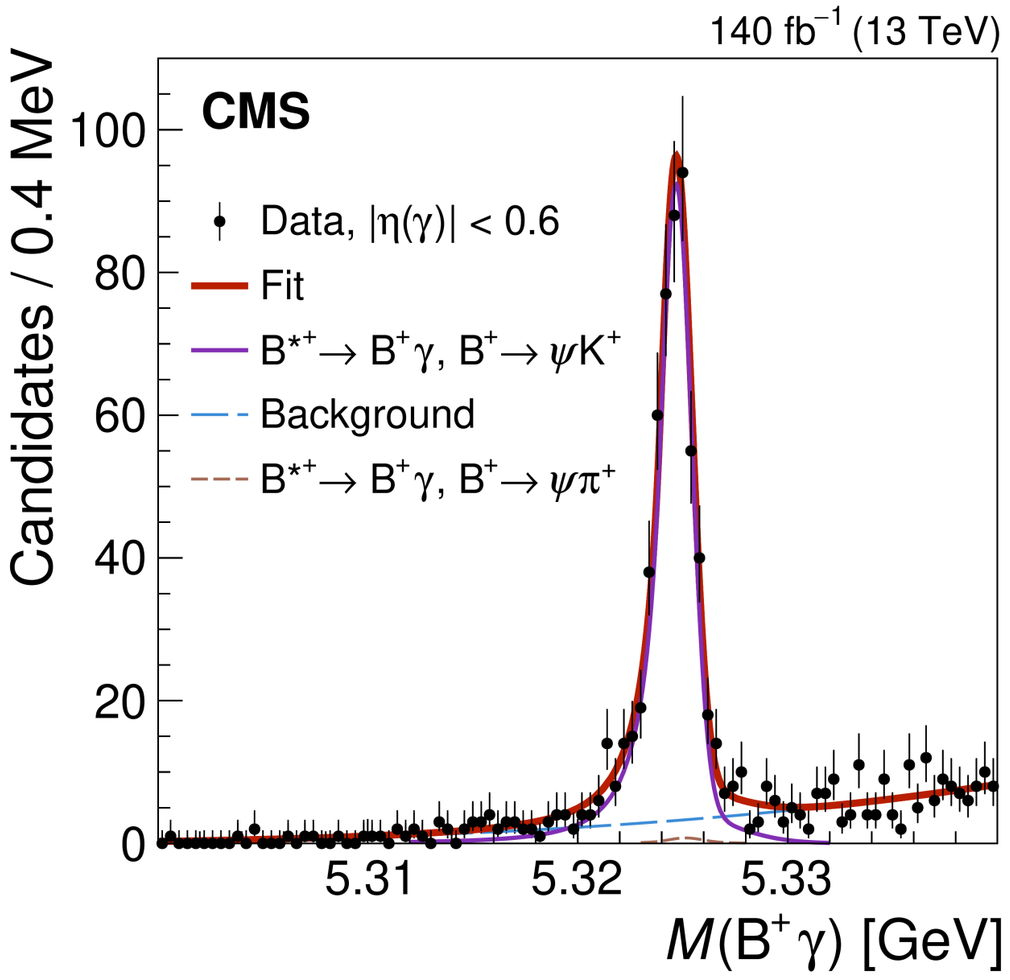
↓

Calibrate the photon momentum

Independent $\pi^0 \rightarrow \gamma\gamma$ sample;
both photons reconstructed as conversions

CMS, PRL 136 (2026) 031902 · converted-photon calibration, Fig. A1b

B* − B: a probe of spin-dependent QCD



B^{*+} → B^{+}γ · 140 fb^{-1} · best-resolution category

B → charmonium + hadrons

Displaced vertex and tight pointing
Reject random combinations

↓

Converted γ + corrected Bγ mass

Reduce the effect of B mass resolution
$M(B\gamma) = m(B\gamma) - m(B) + M_B^{PDG}$

↓

B^{*+}	**B^{*0}**	**B$^{*0}_s$**
Charged	Neutral	Strange

↓

Joint fit in photon-η categories

Separate regions of mass resolution
Random Bγ: smooth background
Misidentified B: peaking templates

CMS, PRL 136 (2026) 031902 · arXiv:2508.05820, Fig. 1a

B* − B splittings at sub-MeV precision

Same quarks in each pair: $J^P = 1^-$ versus 0^-

Quarks	Spin-partner mass difference	ΔM [MeV]
$u\bar{b}$	$\Delta M_u = M(B^{*+}) - M(B^+)$	45.277 ± 0.039 ± 0.027
$d\bar{b}$	$\Delta M_d = M(B^{*0}) - M(B^0)$	45.471 ± 0.056 ± 0.028
$s\bar{b}$	$\Delta M_s = M(B^*_s{}^0) - M(B_s{}^0)$	49.407 ± 0.132 ± 0.041

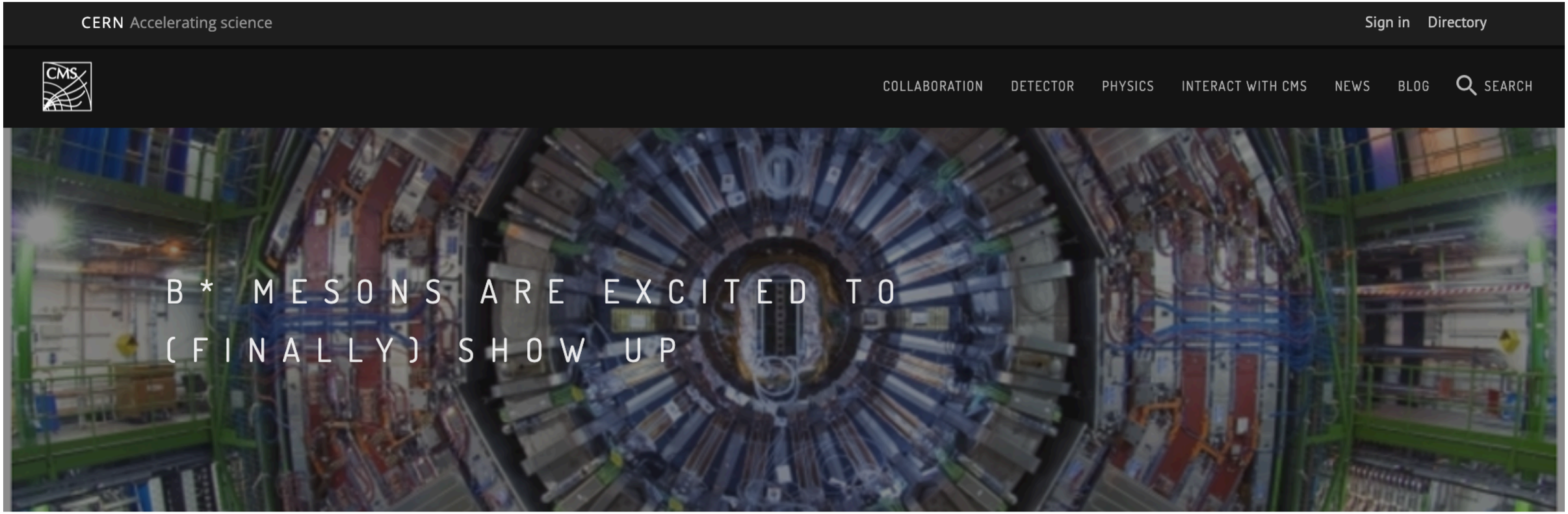
Statistical and systematic uncertainties · CMS Table 2 values
Use the published correlations for flavour differences and ratios.

First exclusive reconstruction of all three flavours.
≈10× better ΔM precision than previous world averages.

Individual ΔM agree with lattice QCD (larger theory errors);
CMS reports $\Delta M_s/\Delta M_{u,d}$ ≈2.5σ above the prediction of Dowdall et al. (2012).

CMS, PRL 136 (2026) 031902 · Table 2 · Lattice: Dowdall et al., PRD 86 (2012) 094510
ATLAS: arXiv:2605.16228

CMS physics briefing: fully reconstructed B* mesons



CMS official news · 5 June 2025 · reporting the PAS

Result later published in **PRL 136 (2026) 031902**

R(J/ψ): comparing decays with τ and μ

$$B_c^+(\bar{b}c) \rightarrow J/\psi(c\bar{c})\, \ell^+ \nu_\ell$$

$$R(J/\psi) = \frac{\mathcal{B}(B_c^+ \rightarrow J/\psi\, \tau^+ \nu_\tau)}{\mathcal{B}(B_c^+ \rightarrow J/\psi\, \mu^+ \nu_\mu)}$$

Same weak coupling, different lepton masses: the SM does not predict R = 1.

Measure the τ mode
CMS reconstructs $\tau \rightarrow 3\pi\nu$ with $J/\psi \rightarrow \mu^+\mu^-$

÷

Measure the μ mode
$B_c \rightarrow J/\psi\, \mu\nu$
Reference decay with a muon

→

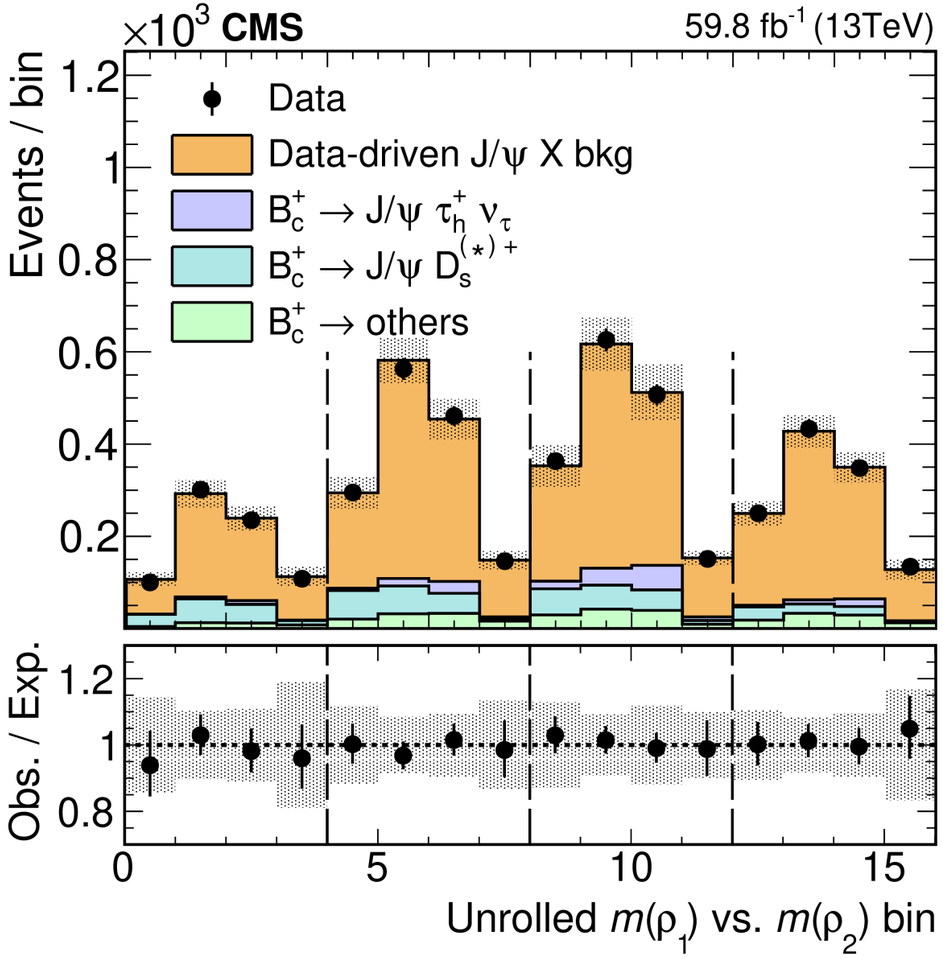
Compare decay rates
Correct for detection efficiency
Test lepton flavour universality

SM expectation: R(J/ψ) = 0.2597 ± 0.0027 · ≈1% precision

Lattice form factors provide the $B_c \rightarrow J/\psi$ strong-interaction input.
Their shapes also enter efficiencies and fit templates.

SM input: HPQCD, PRL 125 (2020) 222003 → PRD 112 (2025) 034503

R(J/ψ): background rejection and signal extraction



2018 signal region · combined fit
4 × 4 mass bins → 16 plotted bins

τ mode: J/ψ + displaced 3π

XGBoost suppresses inclusive-b background
ρ(770) candidates: $(\pi_a^+\pi^-)$ and $(\pi_b^+\pi^-)$
Pair p_T ordering · fit $m(\rho_1)$ vs $m(\rho_2)$
Background: sideband data + MC transfer

+

μ normalization: J/ψ + μ (three muons)

$m(3\mu) < m_{Bc}$, estimated $q^2 < 4.5$ GeV²
Fit L_{xy}/σ_{Lxy}: vertex-displacement significance
Misidentified μ: constrained by control data

↓

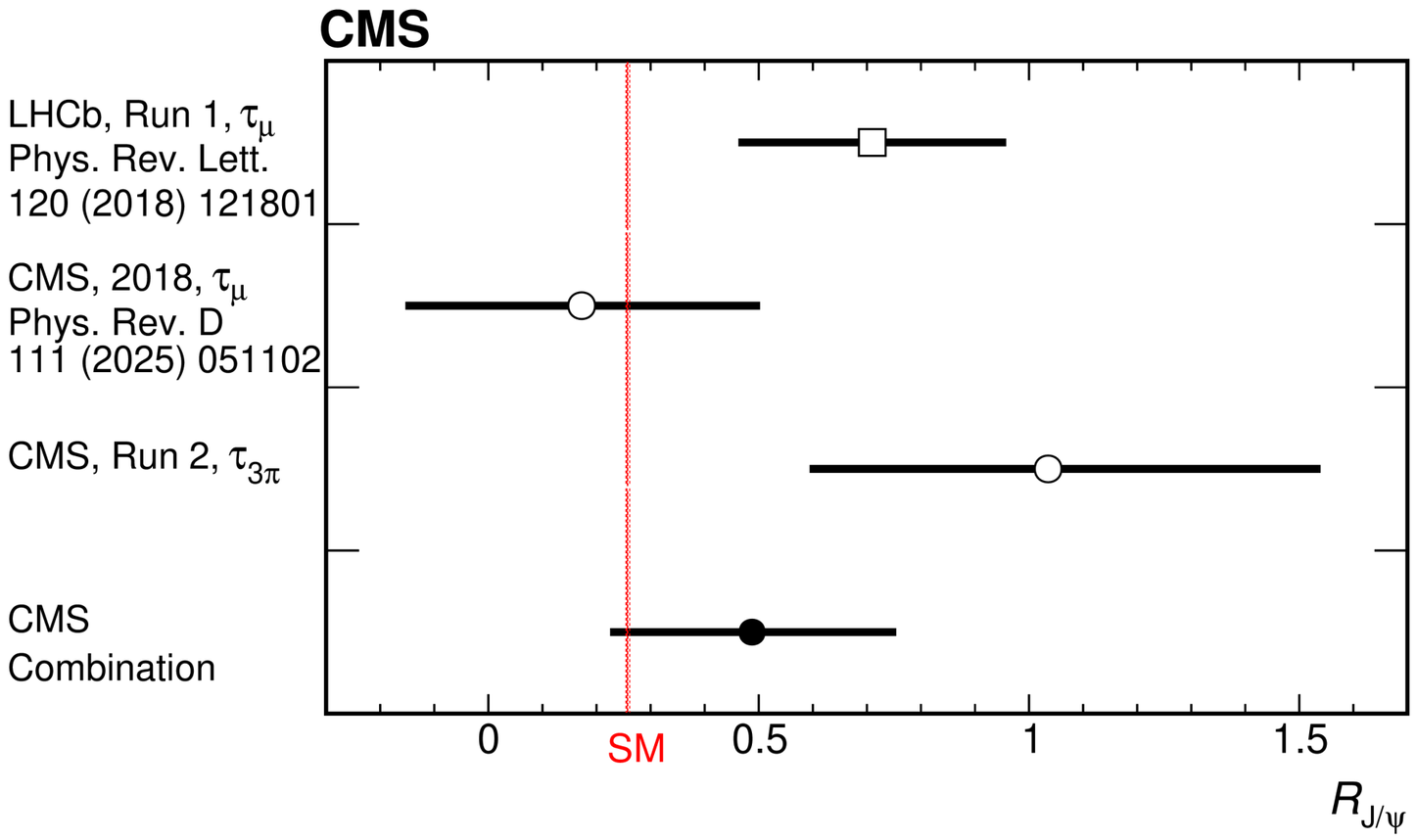
Simultaneous fit → R(J/ψ)

τ → 3πν and τ → μνν share B_c normalization

Hadronic-τ result: **$1.04\ ^{+0.50}_{-0.44}$** (total)

CMS, PRD 113 (2026) L111101 · Fig. 2c · τ: 138 fb⁻¹
μ normalization: CMS, PRD 111 (2025) L051102 · 59.7 fb⁻¹

CMS R(J/ψ): complementary τ channels



Original CMS plot · earlier SM value: 0.258 ± 0.004

CMS combination:
R(J/ψ) = 0.49 ± 0.26
Total uncertainty · ≈53% relative

CMS: first hadronic-τ measurement.
3π vertices and backgrounds complement the μ channel.

LHCb 2026: higher precision
0.51 ± 0.12 ± 0.08
Stat., syst. · τ → μνν · ≈28% total
Both compatible with the SM.

CMS, arXiv:2510.21559, Fig. 3 · LHCb, PRL 137 (2026) 141801

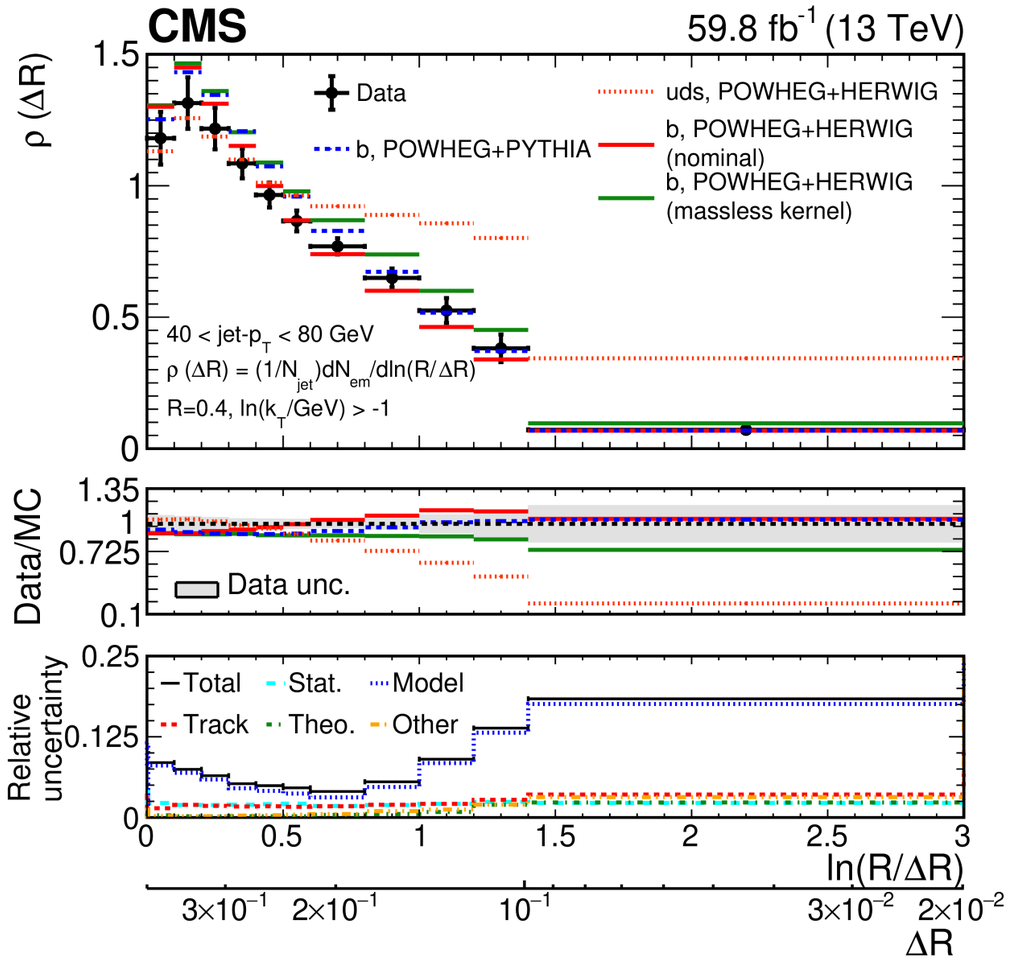
CMS QCD overview: from coupling to hadron formation

How quarks radiate → how hadrons form → how heavy quarks interact

Measurement / physics question	Paper / PAS	CMS analysis · release
α_s and its running Coupling versus energy scale	PLB 868 (2025) 139651	SMP-24-007 · Dec 2024
Bottom-quark dead cone Where does a heavy quark radiate?	arXiv:2608.29412	SMP-25-008 · Aug 2026
Gluon polarization (Zhejiang) Does gluon spin leave a pattern?	arXiv:2603.03689	SMP-25-006 · Mar 2026
Υ(nS) in jets How is a bound state formed inside a jet?	arXiv:2607.25653	SMP-25-005 · Jul 2026
Four-point energy correlations Parton evolution → hadronization	CMS-PAS-SMP-25-009	Preliminary · Aug 2026
$t\bar{t}$ threshold enhancement Slow heavy quarks and the QCD potential	ROPP 88 (2025) 087801 arXiv:2608.19546	TOP-24-007 · Mar 2025 TOP-25-002 · Aug 2026

Institution notes: analysis / presentation roles listed in CLHCP2025.
αs / four-point: overview only. Dates: paper / PAS release, not necessarily first result.

The bottom-quark dead cone: mass changes QCD radiation



Unfolded b-jet radiation · 40 < p_T^{jet} < 80 GeV
Larger ln(R/ΔR) means a smaller emission angle

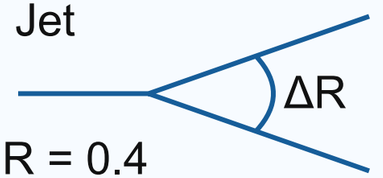
b → b + g: less small-angle radiation
Dead-cone angle $\theta_{dc} \sim m_b/E_b$

$t\bar{t}$ → eμ + jets; tag the other b jet

Displaced vertex selects the probe jet
Transformer: B-decay tracks → B candidate

↓

Undo Cambridge–Aachen clustering

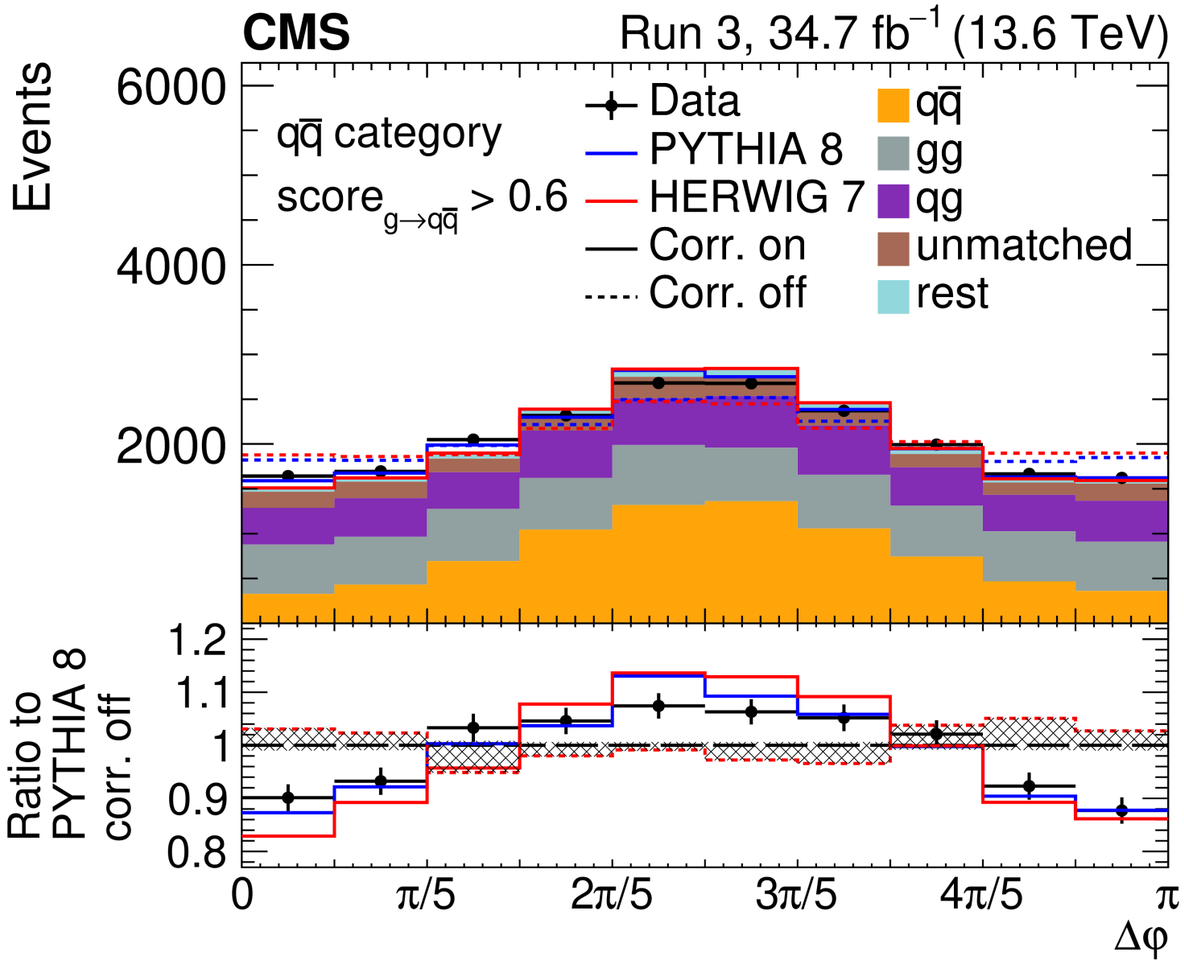


Higher-p_T subjet
emitter proxy

Lower-p_T subjet
emitted-radiation proxy

Result: less radiation at small angles.
4.3σ against the massless HERWIG kernel
40–80 GeV; ln(R/ΔR) > 0.4

Gluon polarization leaves an angular pattern inside jets



Reconstructed Δφ · g → qq̄ enriched category
Solid: spin correlations on; dashed: off

Gluon polarization favours certain relative plane angles.

Example: two successive splittings

$q \to q + g$ → $g \to q' + \bar{q}'$

Plane Π_1 → Plane Π_2

Δφ: angle between Π_1 and Π_2

↓

DNN enriches g → qq̄ splittings

Avoid cancellation with the g → gg pattern

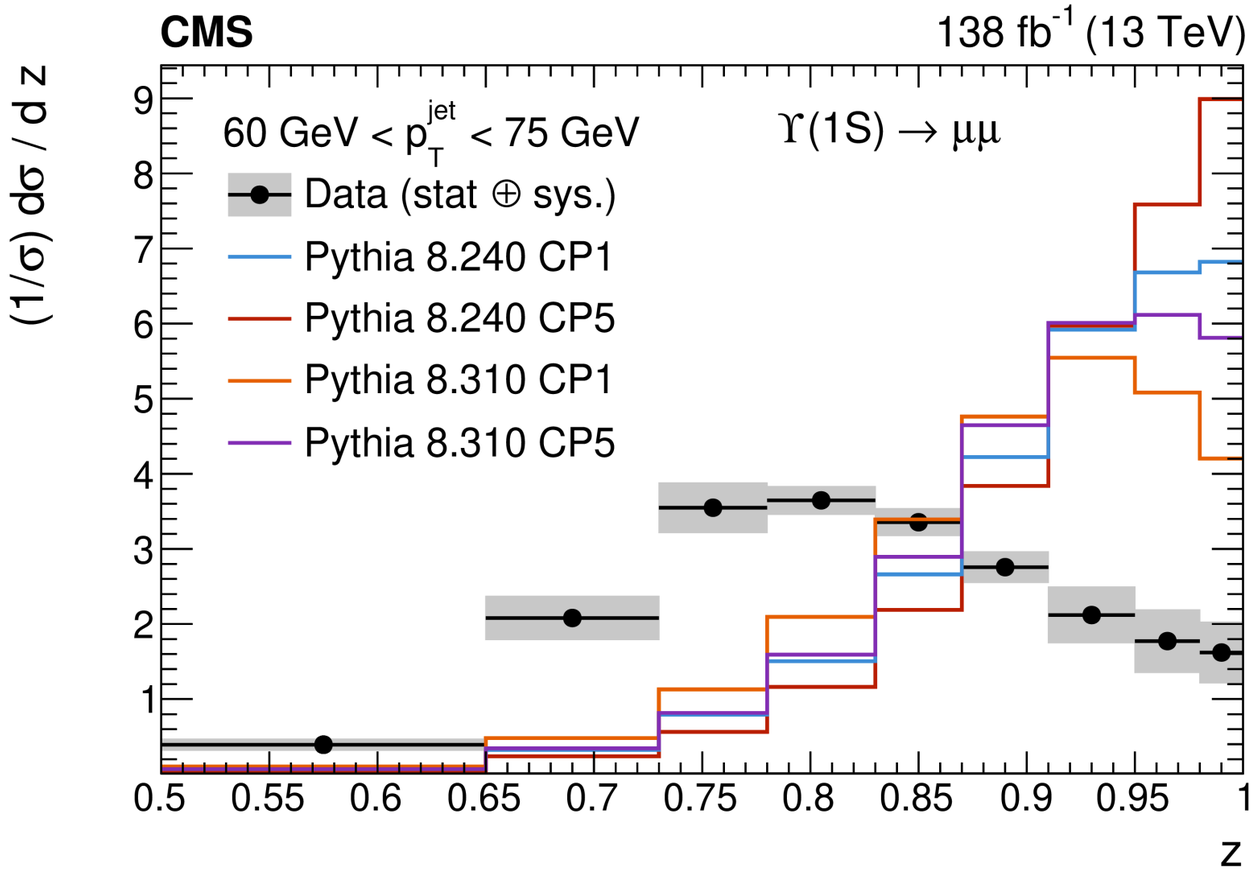
Data favour spin correlations.

6.8σ against PYTHIA correlation-off

Correlation-on: 1.9σ deviation

CMS, SMP-25-006 · arXiv:2603.03689 · submitted to PRL · Fig. 2b

Y (Upsilon) in jets: measuring its share of the momentum



Black points: measured distribution; lines: PYTHIA
Unit-area normalization · grey band: total uncertainty

Y: a $b\bar{b}$ bound state.
Its momentum share tests how it forms.

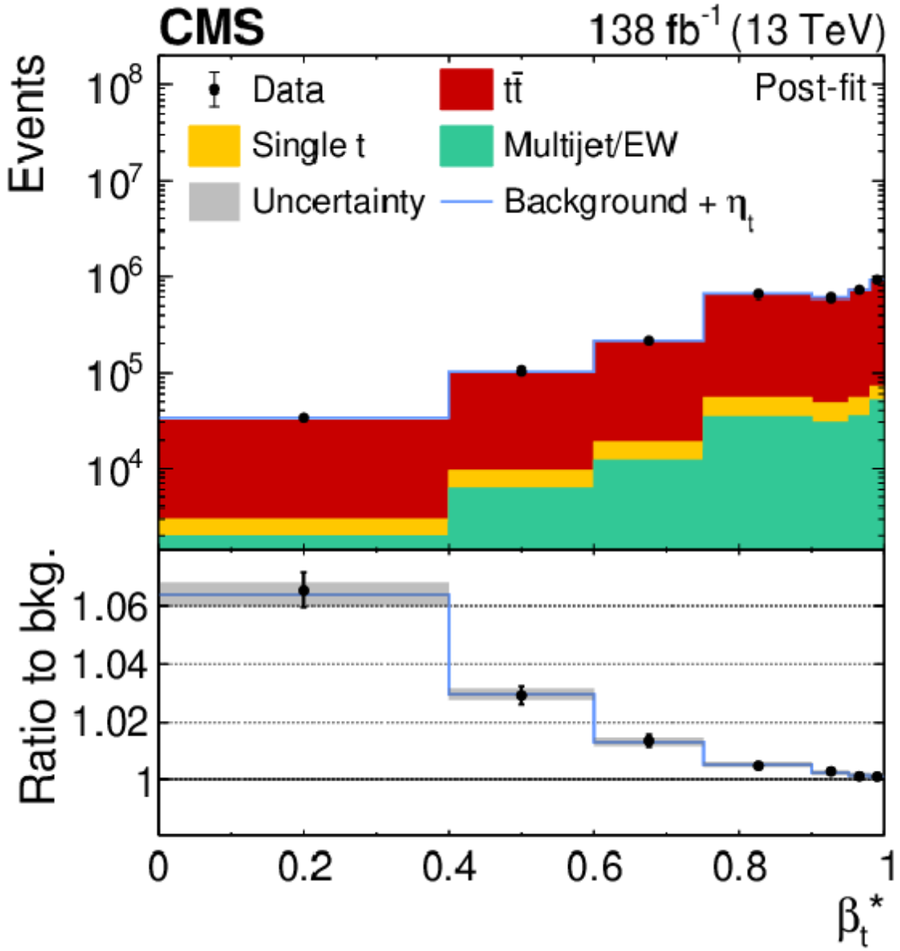
Select $Y \to \mu^+\mu^-$ inside a jet
Fit the dimuon peak in each z bin
Correct for detector effects

↓

$z = (p_Y \cdot p_{jet}) / |p_{jet}|^2$
z = 0.8 means 80% of the jet momentum along its direction is carried by the Y

Large z: data below all PYTHIA curves.
Y carries less jet momentum than predicted.

An excess at the $t\bar{t}$ production threshold



β^*_t: top speed in the other top's rest frame
Near zero: slow pair, close to threshold

Top decays before hadronization.
QCD attraction can enhance production.

One e/μ + ≥4 jets; b tags

NN assigns jets to the two top decays
Fit relative speed β^*_t + two spin angles

↓

Compare two hypotheses

H_0: NNLO QCD + EW $t\bar{t}$ + backgrounds
H_1: H_0 + simplified pseudoscalar η_t (0^-)

Threshold excess over the continuum:
$\sigma(\eta_t)$ = **5.1 ± 0.9 pb**
6.1σ observed vs H_0 (no added η_t)

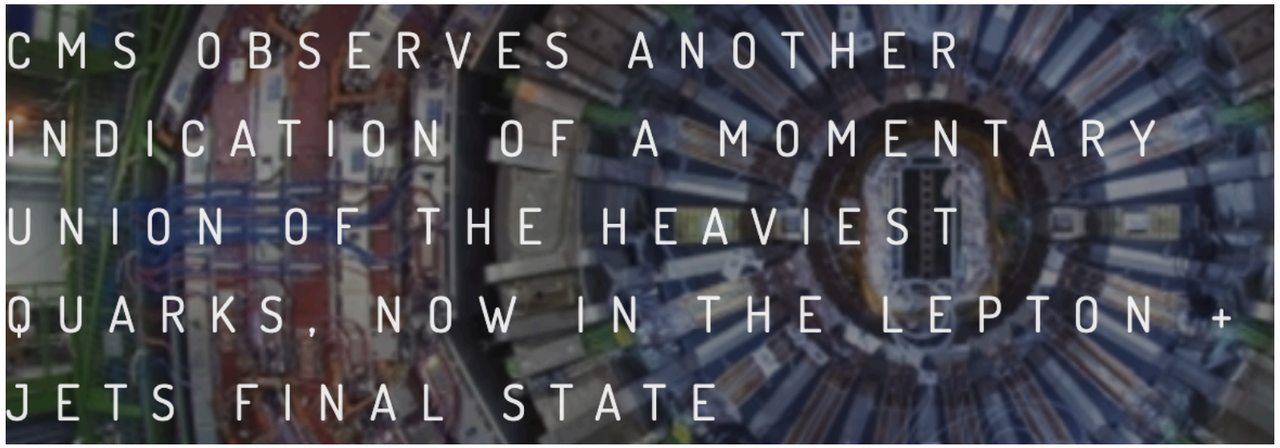
Consistent with quasi-bound toponium;
threshold modelling remains approximate.

CMS, TOP-24-007 · ROPP 88 (2025) 087801 · TOP-25-002 · arXiv:2608.19546, Fig. 12a

CMS Physics Briefings: QCD dynamics



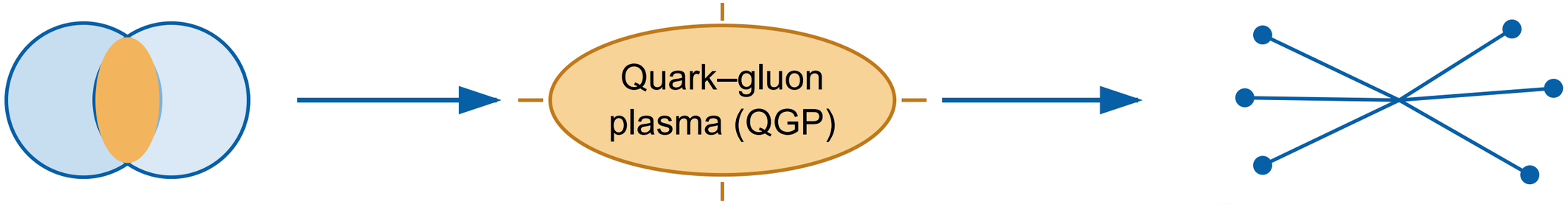
Y in jets · 10 April 2026 · SMP-25-005



Top-pair threshold · 25 March 2026 · TOP-25-002

Original CMS webpage headings: Y in jets · Single-lepton top threshold

Nuclear collisions: from individual probes to QCD matter



Many nucleons interact

Hot matter expands and cools

Flow + modified probes

$\sqrt{s_{NN}}$: energy per nucleon pair

Lead–lead (PbPb)	**$\sqrt{s_{NN}}$**	**Recorded**
Run 2 · 2015–18	5.02 TeV	2.35 nb^{-1}
Run 3 · 2023–26	5.36 TeV	8.16 nb^{-1}

2025: oxygen (OO) and neon (NeNe)
5.36 TeV · Y samples: 8.4 / 0.81 nb^{-1}

Centrality: percentile of inelastic events.
0% = largest overlap; forward energy is the proxy.

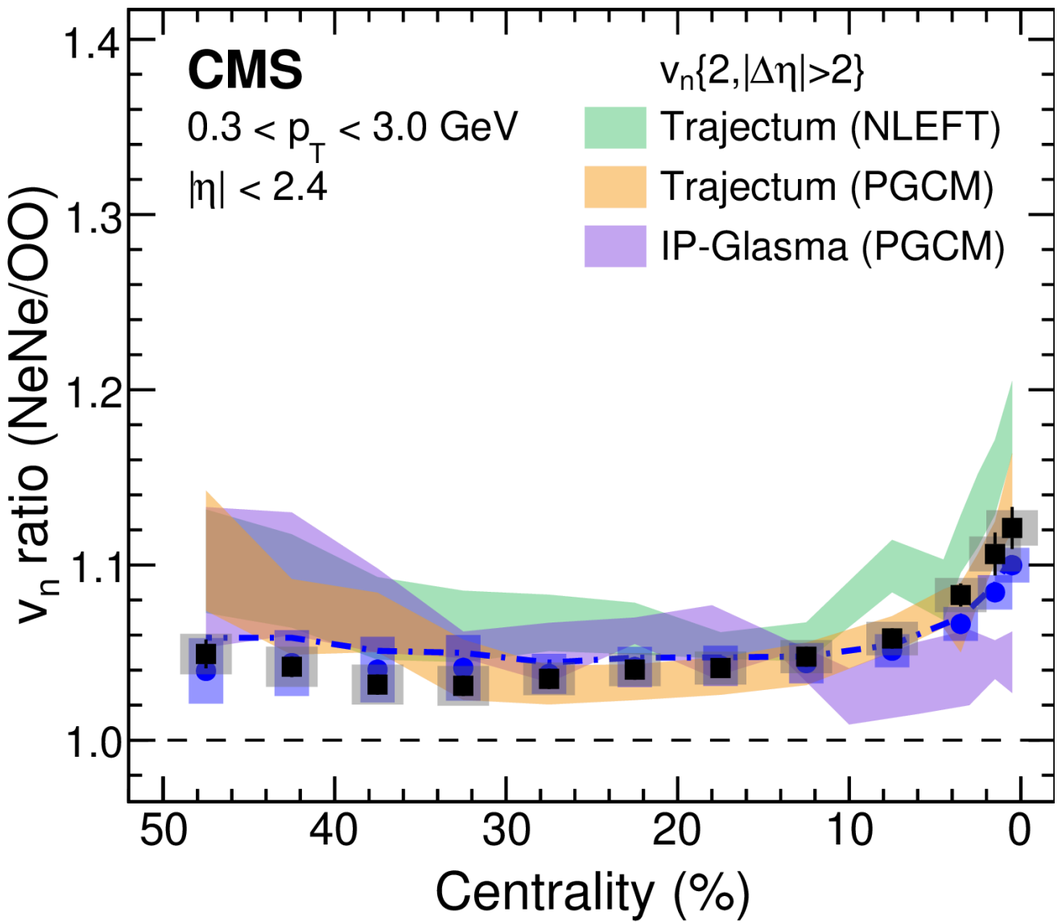
Lattice equation of state → hydrodynamics
Initial geometry and transport also enter;
CMS measures final particles.

Two recent CMS results	**Paper**
OO / NeNe collective flow (Shandong · Fudan) HIN-25-009 · Oct 2025	PRL 137 (2026) 082302
Y suppression in light ions HIN-25-015 · Jul 2026	arXiv:2607.13758 Submitted to PRL

Institution notes: analysis / presentation roles listed in CLHCP2025.

CMS recorded luminosity · CMS heavy-ion review, Phys. Rept. 1115 (2025) 219 · EoS: HotQCD, PRD 90 (2014) 094503

Oxygen and neon: collective motion after a collision



OO: 7 nb^{-1} · NeNe: 0.8 nb^{-1} · 5.36 TeV
Blue: 2-particle v_2; black: 4-particle v_2
Bands: nuclear-structure + hydrodynamic models

v_2 measures an elliptic emission pattern.

Initial geometry → collective expansion
O / Ne: similar sizes; modelled shapes differ.

↓

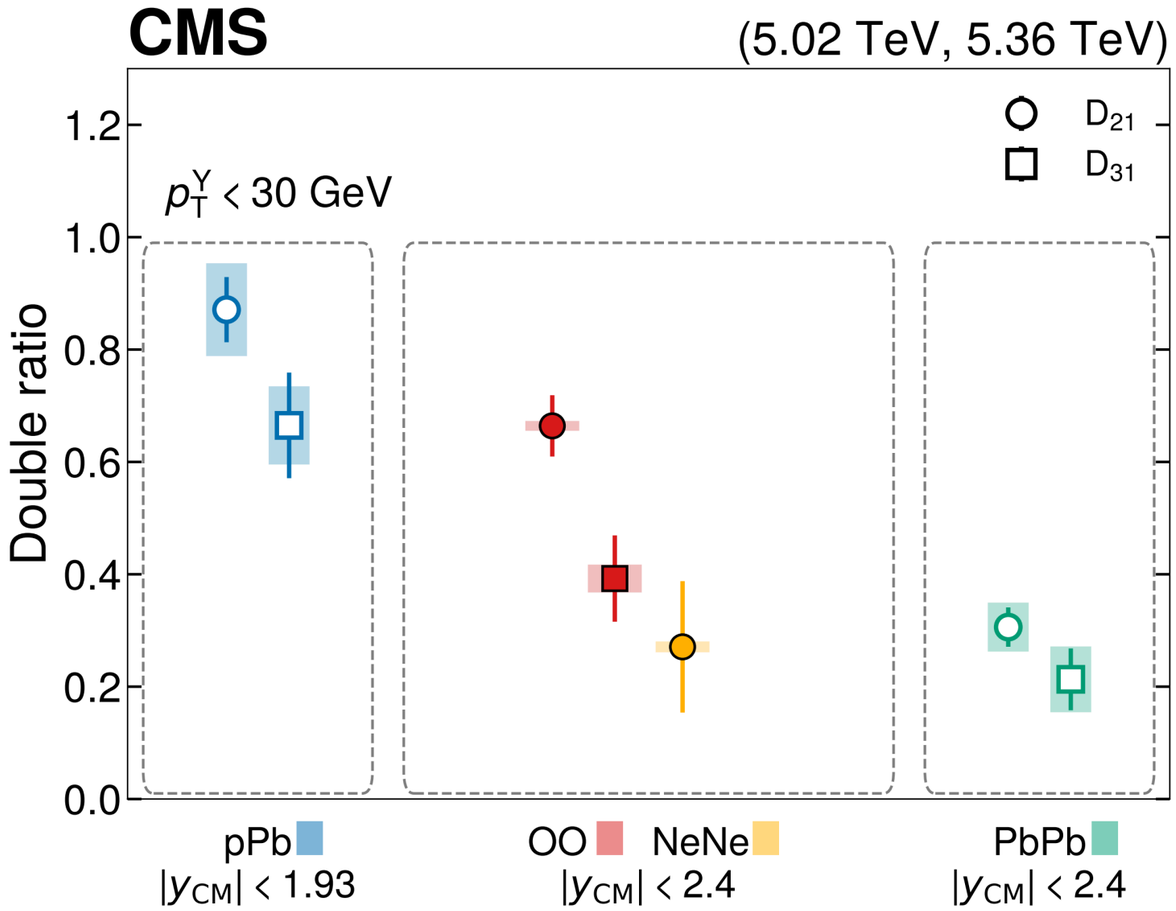
Read the plot: v_2(NeNe) / v_2(OO)
1 = equal v_2; above 1 = stronger in NeNe
Rightward → more head-on collisions

Most central bin: about 10% larger v_2
$v_2\{2\}$(NeNe) / $v_2\{2\}$(OO) = **1.0999**
± 0.0007 (stat) ± 0.0099 (syst)
Centrality-bin centre: 0.5% · $|\Delta\eta| > 2$

Green ↔ orange: nuclear-structure input
Orange ↔ purple: collision modelling
NLEFT: nuclear lattice EFT ≠ lattice QCD

CMS, HIN-25-009 · PRL 137 (2026) 082302 · Fig. 2, left panel · HEPData Table 3 · Dot-dashed: dijet-subtracted

Bottomonium suppression across collision systems



OO: 8.4 nb^{-1} · NeNe: 0.81 nb^{-1}
pp reference: 456 pb^{-1} · all at 5.36 TeV
Earlier pPb / PbPb points: 5.02 TeV

$\Upsilon = b\bar{b}$: a heavy-quark bound state.
2S and 3S are less tightly bound than 1S.

New OO / NeNe; earlier pPb / PbPb

$\Upsilon \rightarrow \mu^+\mu^-$ yields, corrected for detector effects

↓

Compare excited / ground: nuclei vs pp

$D_{n1} = (N_{nS}/N_{1S})_{nuclei} / (N_{nS}/N_{1S})_{pp}$
D = 1: unchanged; D < 1: relative suppression

OO: 2S and 3S each suppressed >5σ vs 1S
3S more than 2S: **3.2σ evidence**
NeNe: 2S/1S double ratio = 0.27
± 0.12 (stat) ± 0.01 (syst)

NeNe: 2S/1S only · energies / acceptances differ.
Compare environments, not a uniform size scan.

CMS, HIN-25-015 · arXiv:2607.13758 (July 2026), Fig. 2a · submitted to PRL

CMS Physics Briefings: light-ion collisions



OO / NeNe flow · 18 September 2025 · HIN-25-009



Y suppression · 29 June 2026 · HIN-25-015

Original CMS webpage headings: Collective flow · Y suppression

Recent CMS highlights in QCD (2025–2026)

Heavy-flavour spectroscopy and weak decays

All-charm: common 2^{++} favoured; J/ψ J/ψ interference and a second charmonium-pair channel.

B*: first exclusive reconstruction of three flavours; hyperfine splittings at sub-MeV precision.

R(J/ψ): a new hadronic-τ channel; the CMS combination is compatible with the SM.

Parton dynamics and hadron formation

Jets reveal **mass-dependent radiation** and test **gluon-spin correlations**.

Υ-in-jet spectra challenge shower models; **$t\bar{t}$ production** shows a threshold enhancement.

QCD matter in light-ion collisions

OO / NeNe flow: sensitivity to nuclear geometry and collective response.

Excited Υ states: suppressed relative to Υ(1S) in light-ion collisions.

CMS combines precision reconstruction and large data sets to probe QCD
from heavy hadrons to jets and hot matter.